High-Redshift Star-Forming Galaxies: Angular Momentum and Baryon Fraction, Turbulent Pressure Effects and the Origin of Turbulence

A. Burkert[1,2], R. Genzel[3], N. Bouché[3], G. Cresci[3], S. Khochfar[3], J. Sommer-Larsen[4,5], A. Sternberg[6], T. Naab[1], N. Förster Schreiber[3], L. Tacconi[3], K. Shapiro[7], E. Hicks[3], D. Lutz[3], R. Davies[3], P. Buschkamp[3], S. Genel[3]

burkert@usm.uni-muenchen.de, genzel@mpe.mpg.de

ABSTRACT

The structure of a sample of high-redshift ($z \sim 2$), rotating galaxies with high star formation rates and turbulent gas velocities of $\sigma \approx 40 - 80$ km/s is investigated. Fitting the observed disk rotational velocities and radii with a Mo, Mao & White (1998) (MMW) model leads to unusually large spin parameters λ in the range of 0.05 to 0.2. In addition, the ratios of disk-to-dark halo masses m_d are extreme and in several cases exceed the cosmic baryon fraction. The galaxies segregate into dispersion-dominated systems with $1 \leq v_{max}/\sigma \leq 3$, maximum rotational velocities $v_{max} \leq 200$ km/s and disk half-light radii $r_{1/2} \approx$ 1-3 kpc and rotation-dominated systems with $v_{max} > 200$ km/s, $v_{max}/\sigma > 3$ and $r_{1/2} \approx$ 4-8 kpc. For the dispersion-dominated sample radial pressure gradients partly compensate the gravitational force, reducing the rotational velocities. Including this pressure effect in the MMW model leads to spin parameters $\lambda \approx 0.035$ and disk mass fractions $m_d \approx 0.1$ that are in good agreement with cosmological expectations. For the rotation-dominated sample, pressure effects are small and better agreement with theoretical expectations can only be achieved if the dark halo mass contribution in the visible disk regime ($2 - 3 \times r_{1/2}$) is much smaller than predicted by the MMW model. We argue that these galaxies can still be embedded in standard cold dark matter halos if the halos did not contract adiabatically in response to disk formation. It is shown that the observed high turbulent gas motions of the galaxies are consistent with a Toomre instability parameter Q=1 which is equal to the critical value, expected for gravitational

[1]University Observatory Munich (USM), Scheinerstrasse 1, 81679 Munich, Germany

[2]Max-Planck-Fellow

[3]Max-Planck-Institut für extraterrestrische Physik (MPE), Giessenbachstr. 1, 85748 Garching, Germany

[4]Dark Cosmology Centre, Niels Bohr Institute, University of Copenhagen, Juliane Marie Vej 30, 2100 Copenhagen, Denmark

[5]Excellence Cluster Universe, Technical University Munich, Boltzmannstr. 2, D-85748 Garching, Germany

[6]School of Physics and Astronomy, Tel Aviv University, Tel Aviv 69978, Israel

[7]Department of Astronomy, Campbell Hall, University of California, Berkeley, CA 94720, USA

disk instability to be the major driver of turbulence. The dominant energy source of turbulence is then the potential energy of the gas in the disk.

Subject headings: cosmology: observations – galaxies: high-redshift – galaxies: individual (BzK-15504) – galaxies: formation – galaxies: evolution – galaxies: halos

1. Introduction

Deep surveys have become efficient in detecting star-forming galaxy populations at z $\sim$ 1.5-3.5, near the peak of cosmic star formation, the assembly of massive galaxies and QSO activity (e.g. Steidel et al. 1996, 2004, Franx et al. 2003, Daddi et al. 2004b). Large samples are now available, based on their rest-frame UV, or optical, magnitude/color properties. These high-redshift galaxies have star formation rates of 10-300 $M_\odot$/yr, with a range of ages (10 Myrs - 3 Gyrs) and stellar masses $M_* \sim 10^9 - 10^{11.5}$ $M_\odot$ (Shapley et al. 2005; Förster Schreiber et al. 2006; Erb et al. 2006b,c; Daddi et al. 2004a,b). They contribute a large fraction of the cosmic star formation activity and stellar mass density at z $\sim$ 2 (Reddy et al. 2005; Rudnick et al. 2006; van Dokkum et al. 2006; Grazian et al. 2007, Perez-Gonzalez et al. 2008). The majority of these galaxies appears to form stars with high rates over a significant fraction of the z $\sim$ 1.5-3 redshift range (Daddi et al. 2007; Noeske et al. 2007). This requires an efficient and semi-continuous replenishment of fresh gas, perhaps delivered by cold flows/streams from the halo (Dekel & Birnboim 2006; Dekel et al. 2009a,b; Kereš et al. 2005; Ocvirk et al. 2008; Genel et al. 2008).

High resolution near-infrared integral field spectroscopy of Hα line emission has shown that most of these high-z star forming galaxies are clumpy and exhibit large ionized gas velocity dispersions of 30-120 km/s (Förster-Schreiber et al. 2006, 2009; Genzel et al. 2006, 2008; Law et al. 2007, 2009; Wright et al. 2007, 2009; van Starkenburg et al. 2008; Stark et al. 2008; Bournaud et al. 2008; Epinat et al. 2009; Cresci et al. 2009). About one third appear to be rotating disks, one third are dispersion dominated systems and one third show clear evidence for interactions and major mergers (Shapiro et al. 2008; Förster Schreiber et al. 2009). The fraction of large, clumpy rotating disks increases with mass. The ratio of the rotational to random velocities ranges between 1 and 6, quite in contrast to z $\sim$ 0 disk galaxies where v/σ $\sim$ 10-20 (Dib et al. 2006). Many high-z disks are turbulent and geometrically thick (e.g. Elmegreen & Elmegreen 2006). Important questions are what drives and maintains these large turbulent velocities and how turbulence is connected to the clumpy disk substructure and the high star formation rates (Immeli et al. 2004a,b; Bournaud et al. 2007, 2008; Dekel et al. 2009a,b; Khochfar & Silk 2008).

In addition to the unusual kinematics and structure of high-redshift disks, their global physical parameters appear to be puzzling and inconsistent with theoretical expectations. Bouché et al. (2007) found that many high-z galaxies lie in a similar part of the rotation velocity versus disk radius plane as late-type z $\sim$ 0 disks (Courteau 2007) which is not expected according to the standard Mo, Mao & White (1998, MMW) model of galactic disk structure. Förster Schreiber et

al. (2009) compared the derived dynamical masses with the stellar masses (from SED analysis) and gas masses (from an application of the Kennicutt-Schmidt star formation relation). They found disk masses that are remarkably and perhaps implausibly high.

The MMW model neglects galactic disk turbulence which is reasonable for present day disks with v/$\sigma \sim 20$. The situation is however different at high redshifts where turbulence can strongly affect the disk structure. This paper discusses the impact of large turbulent motions on the interpretation of the dynamical data of disk galaxies. We show that including turbulent pressure the disk spin parameters and disk mass fractions of dispersion-dominated galaxies are reduced to values that are consistent with theoretical expectations. The situation is different for rotation-dominated galaxies where pressure effects play a minor role. We argue that these galaxies are in better accord with cosmological models if it is assumed that their dark-matter halos did not contract adiabatically. Finally we propose an explanation for why large turbulence might be more common in many high-z disks and what the energy source of turbulence in these disks might be.

2. Rotation Curves of Pressurized, Turbulent Galactic Disks

Let us consider a turbulent galactic gas disk. We analyse its rotational velocity v_{rot} in the midplane, applying the hydrostatic equation

$$\frac{v_{rot}^2}{r} = f_g(r) + \frac{1}{\rho}\frac{dp}{dr} \tag{1}$$

where r is the distance from the galactic center and f_g is the value of the gravitational force. P is the pressure which consists of a turbulent (kinetic) and thermal part, $p = \rho(\sigma^2 + c_s^2)$ with ρ the gas density, σ the characteristic 1-dimensional velocity dispersion of the gas which we assume to be isotropic and c_s its sound speed. We define the zero-pressure velocity curve $v_0(r)$ as the rotational velocity of the gas if pressure gradients are negligible, i.e. dp/dr=0: $v_0^2 \equiv f_g \times r$. Equation (1) then reduces to

$$v_{rot}^2 = v_0^2 + \frac{r}{\rho}\frac{dp}{dr} = v_0^2 + \frac{1}{\rho}\frac{d}{dlnr}\left(\rho\sigma^2\right). \tag{2}$$

Here we have neglected the thermal pressure term as the sound speed is in general much smaller than the turbulent velocity. Equation 2 is the most general form, without specifying the radial dependence of σ and ρ. It demonstrates that a negative radial pressure gradient reduces the rotational velocity of the gas as part of the gravitational force is balanced by the pressure force.

To illustrate the possible importance of pressure effects, let us now assume that σ is independent of r. Then

$$v_{rot}^2 = v_0^2 + \sigma^2 \frac{dln\rho}{dlnr}. \tag{3}$$

If σ is also independent of height z above the disk's equatorial plane, the vertical density distribution is given by the vertical hydrostatic Spitzer solution (Spitzer 1942; Binney & Tremaine 08, chapter 4)

$$\rho(z) = \rho_0 sech^2(z/h) \tag{4}$$

with ρ_0 the density in the midplane (z=0) and

$$h = \frac{\sigma}{\sqrt{2\pi G\rho_0}} \tag{5}$$

the scale height. The total mass surface density $\Sigma(r)$ of such a disk is (Binney & Tremaine 2008)

$$\Sigma = 2\rho_0 h \tag{6}$$

so that

$$\rho_0 = \frac{\pi G\Sigma^2}{2\sigma^2} \tag{7}$$

Inserting ρ_0 from equation 7 into equation 3, the rotation curve in the equatorial plane of a pressurized gas disk is

$$v_{rot}^2 = v_0^2 + 2\sigma^2 \frac{dln\Sigma}{dlnr} \tag{8}$$

For example, an exponential disk profile with scale length r_d gives

$$\Sigma(r) = \Sigma_0 \times \exp\left(-\frac{r}{r_d}\right) \tag{9}$$

Inserting this into equation 8 leads to

$$v_{rot}^2 = v_0^2 - 2\sigma^2 \left(\frac{r}{r_d}\right) \tag{10}$$

For $v_{rot}/\sigma \lesssim 3$ the rotational velocity would be significantly reduced by turbulent pressure effects for $r \gtrsim r_d$. A very similar equation holds for stellar disks as a special form of the Jeans equation

(Binney & Tremaine 2008). Equation 10 was derived for an exponential surface density distribution and a constant velocity dispersion. In general, the situation is more complex as parts of the disk might have constant surface densities while other parts might show a steep gradient. In addition, the velocity dispersion might change with radius. In this case one would have to solve equation (1). The best-resolved high-redshift disk galaxies show constant velocity dispersion profiles and exponentially decreasing Hα-surface brightness distributions of the star-forming gas with scale lengths similar to the stellar disks. For the purpose of this analyses we assume that this holds also for all the other galaxies considered here and adopt equation 10.

3. Galactic Disk Model

We adopt the model by Mo, Mao & White (1998) of an exponential disk, embedded in a NFW (Navarro et al. 1997) dark matter halo with density distribution

$$\rho_{DM}(r) = \frac{4\rho_c}{(r/r_s)(1+r/r_s)^2} \tag{11}$$

where r_s is the halo scale radius and ρ_c is the dark matter density at r_s. The scale radius is related to the virial radius via $r_s = r_{vir}/c$ where c is the halo concentration parameter. The dark halo rotation curve corresponding to equation 11 is

$$v_{DM}^2(r) = V_{vir}^2 \left(\frac{r_{vir}}{r}\right) \frac{ln(1+r/r_s) - (r/r_s)/(1+r/r_s)}{ln(1+c) - c/(1+c)}. \tag{12}$$

High-resolution numerical CDM simulations (e.g. Zhao et al. 2008) show that c depends strongly on cosmological redshift. While c decreases with halo virial mass M_{vir} at low redshifts, the concentration is roughly constant with $c \approx 4$ and independent of halo mass at $z \approx 2$. The halo virial parameters r_{vir} and M_{vir} are related to each other through the virial velocity V_{vir} (Mo, Mao & White 1998)

$$r_{vir}(z) = \frac{V_{vir}(z)}{10H(z)}, \qquad M_{vir}(z) = \frac{V_{vir}^3(z)}{10GH(z)} \tag{13}$$

H is the Hubble parameter that depends on cosmological redshift z:

$$H = H_0 \left[\Omega_\Lambda + (1-\Omega_\Lambda-\Omega_M)(1+z)^2 + \Omega_M(1+z)^3\right]^{1/2}. \tag{14}$$

We adopt a standard ΛCDM cosmology with $H_0 = 73$ km/s/Mpc, $\Omega_M = 0.238$ and $\Omega_\Lambda = 0.762$.

The galactic disk is assumed to follow an exponential surface density profile (equation 9). Its surface density at $r = 0$, Σ_0, is determined by the total disk mass $M_d = m_d M_{vir}$ with m_d the disk mass fraction of the galaxy

$$\Sigma_0 = m_d \frac{M_{vir}}{2\pi r_d^2}. \tag{15}$$

The circular velocity curve of an exponential disk is (Freeman 1970)

$$v_{disk}^2(r) = 4\pi G \Sigma_0 \; r_d y^2 [I_0(y)K_0(y) - I_1(y)K_1(y)] \tag{16}$$

with $y = r/(2r_d)$ and the I_n and K_n denoting the modified Bessel functions (Binney & Tremaine 2008).

In the following we will neglect a bulge because we are interested in the outer disk parts where the bulge contribution to the rotation curve is in general negligible. In addition, several of the best resolved SINS galaxies show no evidence for the presence of a significant bulge component (Genzel et al. 2008). In this case and including adiabatic contraction (Jesseit et al. 2002) of the dark halo, the zero-pressure rotation curve is determined from the implicit equation

$$v_0^2(r) = v_{disk}^2(r) + v_{DM}^2(r') \tag{17}$$

$$r' = r \left[1 + \frac{r \times v_{disk}^2(r)}{r' \times v_{DM}^2(r')} \right]. \tag{18}$$

Given $v_0(r)$ the observed, pressure-corrected rotation curve can now be calculated from equation 2 or 10.

4. Angular Momentum and Baryon Content of High-Z Galaxies

Figure 1 shows the half-light radii $r_{1/2}$ of the SINS high-redshift galaxies versus their maximum rotational velocity v_{max}. We take $r_{1/2}$ instead of the exponential disk scale length as it is independent of any assumption about the light profile. v_{max} is in general a good approximation of the disk's rotational velocities outside of $r_{1/2}$. The SINS galaxies segregate strongly into two distinct classes at a critical value of $v_{max}/\sigma \approx 3$. We therefore empirically define *dispersion-dominated* galaxies (open triangles in figure 1) as objects with $v_{max}/\sigma \leq 3$. For these galaxies turbulent pressure gradients have to be included in the interpretation of the rotation curve. In contrast, for *rotation-dominated* galaxies (filled triangles), defined by $v_{max}/\sigma > 3$, pressure effects are small. Note that σ refers to the intrinsic velocity dispersion in the disk, not to the observed line-of-sight or galaxy-integrated dispersion. Figure 1 shows that most of the dispersion-dominated galaxies have

radii of order 1-3 kpc while the radii of rotationally dominated galaxies are on average a factor of 2-3 larger. In addition, the dispersion-dominated systems have rotational velocities of order 100 km/s while rotation-dominated galaxies rotate with 250 km/s.

The specific angular momentum content of a galactic disk is usually specified by the dimensionless spin parameter (Bullock et al. 2001; Burkert 2009)

$$\lambda = \frac{J}{\sqrt{2} M_{vir} V_{vir} r_{vir}} \tag{19}$$

where J is the total angular momentum of the disk. Numerical simulations show that in the early phases of protogalactic collapse the gas and dark matter are well mixed, acquiring similar λ values (Peebles 1969; Fall & Efstathiou 1980; White 1984). If angular momentum were conserved during gas infall, the resulting disk's angular momentum would be similar to the specific angular momentum of the surrounding dark halo which follows a log-normal distribution with a median of $\lambda = 0.035$ and a dispersion of 0.55 (Bullock et al. 2001; Hetznecker & Burkert 2006). Numerical simulations of galaxy formation find substantial angular momentum loss of the infalling gas component. Galactic disks then should have specific angular momenta that are smaller than those of dark matter halos.

Red lines in figure 1 show the standard MMW model predictions without correcting for pressure effects for a given disk spin parameter λ (red labels), adopting a disk mass fraction of $m_d = 0.1$. The results do not change significantly if m_d is increased to its maximum value which is given by the cosmic baryon fraction $f_b = 0.17$. As we will show below, m_d-values much smaller than 0.1 can be ruled out. $r_{1/2}$ is determined from the known disk scale length: $r_{1/2} = 1.7 \times r_d$. Here we assume that the observed half-light radius, traced by Hα, is similar to the half-mass radius of the disk. According to the red lines most galaxies would have very large spin parameters, $\lambda \approx 0.1 - 0.2$, which is not in agreement with the theoretical expectations of $\lambda \approx 0.035$.

4.1. Dispersion-Dominated Galaxies and the Importance of Pressure Effects

In section 2 we demonstrated that pressure gradients can significantly affect the rotation curves of galaxies when the ratio or rotational velocity to velocity dispersion, characterized e.g. by v_{max}/σ, is sufficiently small.

The blue lines in figure 1 show the correlation between $r_{1/2}$ and v_{max} for a MMW model with pressure correction (equation 10), assuming $v_{max}/\sigma = 2$ which is consistent with the dispersion-dominated galaxy sample. Now, most galaxies lie in the regime $0.02 \leq \lambda \leq 0.05$ which is in good agreement with theoretical expectations. The curves also show that for characteristic spin parameters of 0.035 the disk radii should decrease with decreasing rotational velocities with values of order 1-3 kpc for $v_{max} \approx 100$ km/s, as observed for most of the dispersion-dominated galaxies.

A significant pressure contribution requires larger halo virial masses in order to fit the observed rotational velocities. This in turn increases the virial radii and reduces the spin parameter. In addition, the galaxies' disk mass fractions m_d will be reduced. Figure 2 demonstrates this effect where the symbols represent the sum of the stellar mass (from SED analysis) and gas mass (from an application of the Kennicutt-Schmidt star formation relation) of our galaxy sample, plotted as function of v_{max}. Stars and open triangles correspond to dispersion-dominated systems, filled triangles to rotation-dominated galaxies. One would expect theoretically that the disk mass is not larger than $f_b \times M_{vir}$. The red curves show this limit, $f_b \times M_{vir}$, as function of v_{max} for different values of λ, according to the MMW model. Even for extreme λ values, most SINS galaxies, and especially the dispersion-dominated sample exceed the universal baryon fraction. The blue curves show the situation when pressure effects are included, adopting $v_{max}/\sigma = 2$. Now the observed disk masses correspond to MMW models with disk mass fractions m_d that are smaller than f_b for reasonable spin parameters. Adopting $\lambda \approx 0.035$ most pressure-supported SINS galaxies, represented by the open triangles, have disk mass fractions $m_d \approx 0.03 - 0.15$, with a mean of 0.1.

Figure 2 shows that there exists a sharp upper boundary for galaxies with $v_{max}/\sigma \geq 2$ that is traced by the uppermost thick blue curve, corresponding to $\lambda = 0.2$. The dashed blue curve next to it corresponds to $\lambda = 0.1$ and demonstrates that for high spin values the correlation between v_{max} and the virial mass is not very sensitive to λ. For objects to lie above this limit, either λ must be unreasonably high or v_{max}/σ must be smaller than 2. There indeed exists a subgroup of dispersion-dominated systems, that clearly lie above this boundary. The stars in figure 2 show all galaxies with $v_{max}/\sigma < 1.5$ which matches this group of outliers very well, consistent with the theoretical expectations that due to their extreme velocity dispersions, the rotational velocities of these objects have been shifted to lower values than expected for $v_{max}/\sigma = 2$.

4.2. Rotation-Dominated Galaxies and Adiabatic Halo Contraction

The rotation-dominated SINS sample is characterized by average values of $v_{max}/\sigma \approx 5$. The problem of unusually high spin parameters and baryon fractions therefore cannot be solved by consideration of pressure gradients. A typical representative of this group is BzK-15504 which has been observed with high angular resolution (Genzel et al. 2006). BzK-15504 is an actively star-forming $z = 2.4$ galaxy with an observed total disk mass of $M_d \approx 1.4 \times 10^{11} M_\odot$. The radial H$\alpha$ gas surface brightness and the rest-frame optical stellar light distributions are both consistent with an exponential profile with scale length of 4.1 kpc.

The observed line width indicates irregular gas motions of $\sigma \approx 45 \pm 20$ km/s that are constant throughout the disk outside of the central 3 kpc where a bar and an AGN strongly affect the gas kinematics. Its maximum rotational velocity is $v_{max} = 258$ km/s, so that $v_{max}/\sigma = 5.7$. The dark matter virial mass is not well constrained. Its minimum value is however given by $M_{vir} \geq M_d/f_b \approx 8 \times 10^{11} M_\odot$.

The dotted red and blue curves in the left panel of figure 3 show the disk and dark matter rotation curves, respectively, adopting a MMW model and the above mentioned disk parameters. Both components are equally important with peak rotational velocities at r $\approx$ 10 kpc of 250 km/s and 280 km/s. The upper black curve shows the resulting combined rotation curve, neglecting pressure. It peaks at 370 km/s and is clearly inconsistent with the observations (red open circles) that peak at $\sim$ 260 km/s. Including the turbulent pressure gradient with σ = 45 km/s does not significantly change the rotation curve (black points).

Is this disagreement an observational problem? The uncertainty in the measured disk velocity dispersion is large, of order 20 km/s. However a dispersion of even 65 km/s (dashed black curve in the left panel of figure 3) makes no big difference given the large rotational velocities of 370 km/s. The uncertainties in the determination of the rotation curve are of order 25 km/s, too small compared with the observed disagreement of almost 100 km/s. The only possible solution appears to be a strong reduction of either the baryonic or the dark matter mass within the inner 10 kpc. A test calculation shows that the baryonic disk mass would have to be reduced by a factor of 2 to $\sim 7 \times 10^{10} M_{\odot}$ for a pressure corrected MMW model to fit the observations. The estimates of the stellar and gas masses are subject to many uncertainties and systematics. SED fitting for BzK-15504 using the Maraston (2005) models yields stellar masses of $M_* = 9.4(+2.6/-0.2) \times 10^{10} M_{\odot}$ and gas masses of $M_{gas} = 3.1(+0.6/-0.6) \times 10^{10} M_{\odot}$ using the Schmidt-Kennicutt relation from Bouché et al. (2007) and the same extinction towards HII regions as towards the stars. The gas masses would be a factor of 2 higher if the extinction towards HII regions is a factor of 2 higher than towards stars (Calzetti et al. 2004). The best-fit Bruzual & Charlot (2003) model gives $M_* = 10.9(+2.7/-0.1) \times 10^{10} M_{\odot}$ and $M_{gas} = 2.8(+0.5/-0.6) \times 10^{10} M_{\odot}$. Unless the stellar initial mass function is bottom-light or top-heavy it therefore seems difficult to decrease substantially the baryonic disk mass of the galaxy.

The second possibility is a smaller dark halo mass in the disk region. One critical assumption that enters the MMW model is that the dark halo reacts to the formation of the galactic disk by contracting adiabatically. The right panel of figure 3 shows the situation for a MMW model, neglecting dark halo contraction. A comparison with the left panel demonstrates the strong effect of adiabatic contraction. Although the dark matter virial parameters in both cases are the same, without adiabatic contraction the contribution of the dark halo (blue dashed line) within the disk region is small, leading to much better agreement of the model with the observations, especially if we take into account a turbulent pressure, corresponding to a velocity dispersion of σ = 65 km/s (upper dashed black line), that is still within the observed uncertainties.

The problem discussed for BzK 15504 exists for all rotation-dominated galaxies that are represented in the figures 1 and 2 by black filled triangles. Due to their large values of $v_{max}/\sigma \approx 5$ the effect of pressure gradients is small. The galaxies are therefore represented well by the red lines in both figures which indicate spin parameters and mass fractions that are unrealistic. The solid black lines in both figures show the strong effect of neglecting adiabatic dark halo contraction. The spin parameters of the models that fit the rotation-dominated galaxies are now $\sim$0.07 which is still

high, however much more reasonable than the previous values of 0.12. Adopting $\lambda = 0.07$, figure 2 shows that in the case of negligible dark halo contraction most of the rotation-dominated galaxies have disk mass fractions that a smaller than the cosmic baryon fraction with values of the order 0.1.

5. Origin of Gas Turbulence in High-Redshift Disk Galaxies

The MMW models also provide insight into the origin of the observed gas turbulence. Let us propose that the main driver of clumpiness and turbulence in gas-rich high-redshift disks is gravitational disk instability. Then we expect gas-rich disks to stay close to the gravitational stability line because of the following reason. A disk that is kinematically too cold with small velocity dispersions is highly gravitationally unstable. Gravitational instabilites generate density and velocity irregularities that drive turbulence and heat the system kinematically. As a result, the gas velocity dispersion increases till it approaches the stability limit where kinetic driving by gravitational instabilities saturates. A disk with even higher velocity dispersions would be stable. Here the turbulent energy would dissipate efficiently and the velocity dispersion would decrease again until it crosses the critical velocity dispersion limit where gravitational instabilities become efficient again in driving turbulent motions. In summary, galactic disks should settle close to the gravitational stability line that is determined by the Toomre criterion (Toomre 1964; Wang & Silk 1994)

$$Q \equiv \frac{\kappa}{\pi G}\left(\frac{\Sigma_g}{\sigma_g}+\frac{\Sigma_*}{\sigma_*}\right)^{-1} \leq Q_c. \tag{20}$$

κ is the epicyclic frequency that is related to the local angular circular velocity Ω at radius r through $\kappa^2 = rd\Omega^2/dr + 4\Omega^2$ and Q_c is the critical value which is of order unity (Goldreich & Lynden-Bell 1965; Dekel et al. 2009b). Σ_* and σ_* are the stellar surface density and velocity dispersion, respectively. As a test, let us focus again on BzK 15504. As most of the stars in BzK 15504 are likely to have formed during the presently observed star burst we can assume that the stellar velocity dispersion is similar to the observed turbulent gas velocity, i.e. $\sigma_* \approx \sigma_g$. In addition, the observations show that both components have similar exponential disk scale lengths. If the disk is close to the instability line, its turbulent gas velocity dispersion at any point r is then

$$\sigma = \frac{\pi G \Sigma}{\kappa} \tag{21}$$

where $\Sigma(r)$ is the local baryonic (gas+stars) disk surface density. The lower black dot-dashed curve in the right panel of figure 3 shows the predicted gas velocity dispersion for BzK-15504. It is indeed almost independent of radius and within the uncertainty in agreement with the observed, radially constant value of 45 ± 25 km/s. We thus conclude that BzK-15504 is a marginally unstable

star-forming disk (Genzel et al. 2006), driven by gravitational instabilities.

We calculated the velocity dispersion profile for all SINS galaxies with $v_{max}/\sigma \geq 2$ using a pressure corrected MMW model and neglecting adiabatic halo contraction. The disk mass was taken from the observed stellar and gas masses. The dark halo mass was constrained by fitting the observed maximum velocity of the galaxies. In all cases the theoretically derived velocity dispersion σ_{theo}, adopting equation 21, was almost constant within 1 and 2 disk scale radii. Figure 4 compares σ_{theo} with the observed velocity dispersion σ_{obs}. Dispersion-dominated (open triangles) and rotation-dominated (filled triangles) systems have similar gas velocity dispersions, indicating that the difference in v_{max}/σ is due to a difference in rotational velocities and not a result of differences in the turbulent gas velocity. Despite the large uncertainties, the theoretical and observed velocity dispersions agree well, strengthening the suggestion that gravitational instabilities are the major driver of turbulence in high-redshift star-forming galaxies.

6. Summary and Discussion

In this paper we show that pressure gradients in turbulent galactic disks may significantly affect their rotation curves. This effect is well-known for thick stellar disks, leading e.g. to an asymmetric drift of kinematically hot stellar populations in the Galaxy (Binney & Tremaine 2008). A similar effect is found in models of dust growth in protoplanetary disks where dust particles on ballistic orbits rotate faster than the disk gas which rotates sub-Keplerian due to pressure gradients, leading to fatal dust migration into the central star (e.g. Takeuchi & Artymowicz 2001).

We analyse the SINS sample of dispersion-dominated high-redshift star-forming galaxies. Including pressure effects and adopting an exponential gas disk with scale length similar to the stellar disk, the models can explain the properties of the dispersion-dominated SINS galaxies very well, with disk spin parameters of $\lambda \approx 0.035$ and disk mass fractions of $m_d \approx 0.1$, in good agreement with cosmological expectations. The strong pressure affect on the structure of dispersion-dominated galaxies depends critically on the assumption of a gas pressure gradient in their disks. The best resolved SINS galaxies indicate a radially constant turbulent velocity dispersion and an exponential decline of the surface density of star-forming gas with scale length similar to the stellar disk. It is however not clear whether all high-redshift galaxy have such a structure. More high-resolution observations are required in order to clarify this point.

For rotation-dominated galaxies, defined by $v_{max}/\sigma \geq 3$ with typical values of 5, pressure gradients cannot strongly affect the rotational velocities. Analysing as a test case the galaxy BzK 15504 we show that its rotation curve allows no significant contribution of dark matter within the visible disk region. This can be achieved with a standard NFW halo that did not contract adiabatically in response to the formation of the galactic disk. In this case, the MMW fit leads to disk spin parameters in the range of $0.05 \leq \lambda \leq 0.1$ with $m_d \approx 0.1$ for the rotation-dominated sample. The baryon fraction is reasonable. The spin parameters are however still high indicating a

more complex relationship between disk and halo specific angular momentum as discussed e.g. by Sales et al. (09).

The mechanisms that could have suppressed dark halo contraction are not well understood yet. Gnedin et al. (2004) and Gustafsson et al. (2006) argue that the circular orbit adiabatic contraction model (Barnes & White 1984) considerably overestimates the amount of dark matter contraction. The numerical simulations of Jesseit et al. (2002) however find good agreement with the analytical expression. The dark matter mass fraction in the disk region could also be reduced if one assumes cored dark matter halos (Burkert 1995; Salucci & Burkert 2000), resulting e.g. from dark matter annihilation or dark matter particle scattering. Another possibility is heating of the kinematically cold dark matter cusps e.g. by gravitational interaction with infalling gas clumps or massive clumps in the turbulent disk (Mashchenko et al. 2006). Abadi et al. (2009) compare cosmological dark-matter-only simulations with a second set where a baryonic gas component, star formation and stellar feedback is added. They find that with baryons the core densities of dark matter halos are strongly reduced, demonstrating that dark halo Although not required in order to produce reasonable spin parameters and disk mass fractions, the processes that suppressed adiabatic halo contraction in rotation-dominated galaxies might also have been active in dispersion-dominated systems. In this case, most dispersion-dominated systems would be characterized by even smaller spin parameters $\lambda < 0.035$ and lower disk mass fractions $m_d < 0.1$.

We have analysed the origin of turbulence in high-redshift disk galaxies. Assuming that the disks are marginally unstable we can explain the observed velocity dispersion. This indicates that turbulence is driven and regulated by gravitational instabilites, combined with turbulent energy dissipation. We argue that in this case galactic disks will tend to stay close to a state of marginal gravitational stability which for gas-rich disks corresponds to a velocity dispersion of order 40 - 80 km/s. The energetic source of the turbulent driver is then the potential energy of the disks' gas which, coupled with viscous forces releases potential energy by spiraling inwards, generating at the end bulge-dominated galaxies as suggested e.g. by Elmegreen et al. (2008) and Dekel et al. (2009a,b). Other energy sources like stellar feedback or accretion energy from infalling gas would then play a minor role. For if these processes were dominating, the velocity dispersion would most likely differ from the value expected for a marginally unstable disk. Note, that within the framework of this scenarion the observed velocity dispersion is a signature of global gas motions that affect the global disk structure and not just the result of local stellar energy feedback, generating HII regions and driving local outflows of ionized gas. This conclusion is consistent with the finding of Elmegreen & Elmegreen (2006) that the stellar z-scale heights of high-redshift star-forming galaxies are of order 1 kpc, which translates to a global velocity dispersion of order 50 km/s. Whether gas-rich galactic disks naturally evolve towards a state of marginal stability through gravitational driving of turbulence, combined with turbulent energy dissipation is an interesting question that should be explored in greater details.

Acknowledgments: A.B. is partly supported by a Max-Planck-Fellowship. This work was supported by the DFG Cluster of Excellence "Origin and Structure of the Universe". The Dark

Cosmology Centre is funded by the Danish National Research Foundation.

REFERENCES

Abadi, M.G., Navarro, J., Fardal, M., Babul, A. & Steinmetz, M. 2009, astro-ph/0902.2477

Barnes, J. & White, S.D.M. 1984, MNRAS, 211, 753

Binney, J. & Tremaine, S. 2008, Galactic Dynamics (Princeton, NJ, Princeton University Press, 2008)

Bouché, N. et al. 2007, ApJ, 671, 303

Bournaud, F., Elmegreen, B.G. & Elmegreen, D.M. 2007, ApJ, 670, 237

Bournaud, F. et al. 2008, A&A, 486, 741

Bruzual, G. & Charlot, S. 2003, MNRAS, 344, 1000

Bullock, J.S. et al. 2001, ApJ, 555, 240

Burkert, A. 1995, ApJ, 447, L25

Burkert, A. 2009, in The Galaxy Disk in Cosmological Context, IAU Symposium 254, 437

Calzetti, D., Harris, J., Gallagher, J.S., Smith, D.A., Conselice, C.J., Homeier, N. & Kewley, L. 2004, AJ, 127, 1403

Courteau et al. 2007, ApJ, 671, 203

Cresci, G. et al. 2009, ApJ, in press.

Daddi, E. et al. 2004a, ApJ, 600, L127

Daddi, E., Cimatti, A., Renzini, A., Fontana, A., Mignoli, M., Pozetti, L., Tozzi, P. & Zamorani, G. 2004b, ApJ, 617, 746

Daddi, E. et al. 2007, ApJ, 670, 156

Dekel, A. & Birnboim, Y. 2006, MNRAS, 368, 2

Dekel, A. et al. 2009a, Nature, 457, 451

Dekel, A., Sari,, R. & Ceverino, D. 2009b, submitted, astro-ph/0901.2458

Dib, S., Bell, E. & Burkert, A. 2006, ApJ, 638, 797

Elmegreen, D.M. & Elmegreen, B.G. 2006, ApJ, 650, 644

Elmegreen, D.M., Elmegreen, B.G., Ravindranath, S. & Cox, D.A. 2007, ApJ, 658, 763

Elmegreen, B.G., Bournaud, F. & Elmegreen, D.M. 2008, ApJ, 688, 67

Epinat et al. 2009, submitted to MNRAS, astro-ph/0903.1216

Erb, D. K., Steidel, C. C., Shapley, A. E., Pettini, M., Reddy, N. A. & Adelberger, K. L. 2006b ApJ, 646,107

Erb, D. K., Steidel, C. C., Shapley, A. E., Pettini, M., Reddy, N. A. & Adelberger, K. L. 2006c, ApJ, 647,128

Fall, S.M. & Efsthatiou, G. 1980, MNRAS, 193, 189

Förster Schreiber, N. M. et al. 2006, ApJ, 645, 1062

Förster Schreiber, N. M. et al. 2009, ApJ, in press

Franx, M., et al. 2003, ApJ, 587, L79

Freeman, K.C. 1970, ApJ, 160, 811

Genel, S. et al. 2008, ApJ, 688, 789

Genzel, R. et al. 2006, Nature, 442, 786

Genzel, R. et al. 2008, ApJ, 687, 59

Gnedin, O,Y., Kravtsov, A.V., Klypin, A.A. & Nagai, D. 2004, ApJ, 616, 16

Goldreich, P. & Lynden-Bell, D. 1965, MNRAS, 130, 125

Grazian, A. et al. 2007, A&A, 465, 393

Gustafsson, M., Fairbairn, M. & Sommer-Larsen, J. 2006, Phys. Rev. D., 74, 3522

Hetznecker, H. & Burkert, A. 2006, MNRAS, 370, 1905

Immeli, A., Samland, M. Gerhard, O. & Westera, P. 2004a, A&A, 413, 547

Immeli, A., Samland, M. Westera, P. & Gerhard, O. 2004b, ApJ, 611, 20

Jesseit, R., Naab, T. & Burkert, A. 2002, ApJ, 571, 89

Khochfar, S. & Silk, J. 2008, submitted to ApJL, astro-ph/0812.1183

Kereš D., Katz, N., Weinberg, D.H. & Davé, R. 2005, MNRAS, 363, 2

Law, D., Steidel, C.C., Erb, D.K., Larkin, J.E., Pettini, M., Shapley, A.E. & Wright, S.A. 2007, ApJ, 669, 929

Law, D. et al. 2009, ApJ, submitted

Maraston, C. 2005, MNRAS, 362, 799

Mo, H.J., Mao, S. & White, S.D.M. 1998, MNRAS, 295, 319

Mashchenko, S., Couchman, H.M.P. & Wadsley, J. 2006, Nature, 442, 7102

Navarro, J.F., Frenk, C.S. & White, S.D.M. 1997, ApJ, 490, 493

Noeske, K.G. et al. 2007, ApJ, 660, L43

Ocvirk, P., Pichon, C. & Teyssier, R. 2008, MNRAS, 390, 1326

Peebles, P.J.E. 1969, ApJ, 155, 393

Pérez-Gonzalez, P.G. et al. 2008, ApJ, 675, 234

Reddy, N. A., Erb, D. K.,Steidel, C. C., Shapley, A. E., Adelberger, K. L., & Pettini, M. 2005, ApJ, 633, 748

Rudnick et al. 2006, ApJ, 650, 624

Sales, L.V. et al. 2009, submitted to MNRAS Letters, astro-ph/0905.3554

Salucci, P. & Burkert, A. 2000, ApJ, 537, 9

Shapiro, K.L. et al. 2008, ApJ, 682, 231

Shapley, A.E. et al. 2005, ApJ, 626, 698

Spitzer, L. 1942, ApJ, 95, 329

Stark et al. 2008, Nature, 455, 775

Steidel, C.C., Shapley, A.E., Pettini, M., Adelberger, K.L., Erb, D.K., Reddy, N.A., & Hunt, M.P. 2004, ApJ, 604, 534

Takeuchi, T. & Artymowicz, P. 2001, ApJ, 557, 990

Toomre, A. 1964, ApJ, 139, 1217

van Dokkum, P.G. et al. 2006, ApJ, 638, L59

Van Starkenburg, L., van der Werf, R.P., Franx, M., Labb'e, I., Rudnick, G. & Wuyts, S. 2008, A&A, 488, 99

Wang, B. & Silk, J. 1994, ApJ, 427, 759

White, S.D.M. 1984, MNRAS, 286, 38

Wright, S.A. et al. 2007, ApJ, 658, 78

Wright, S.A. et al. 2009, ApJ, 699, 421

Zhao, D.H., Jing, Y.P., Mo, H.J. & Boerner, G. 2008, submitted to ApJ, astro-ph/0811.0828

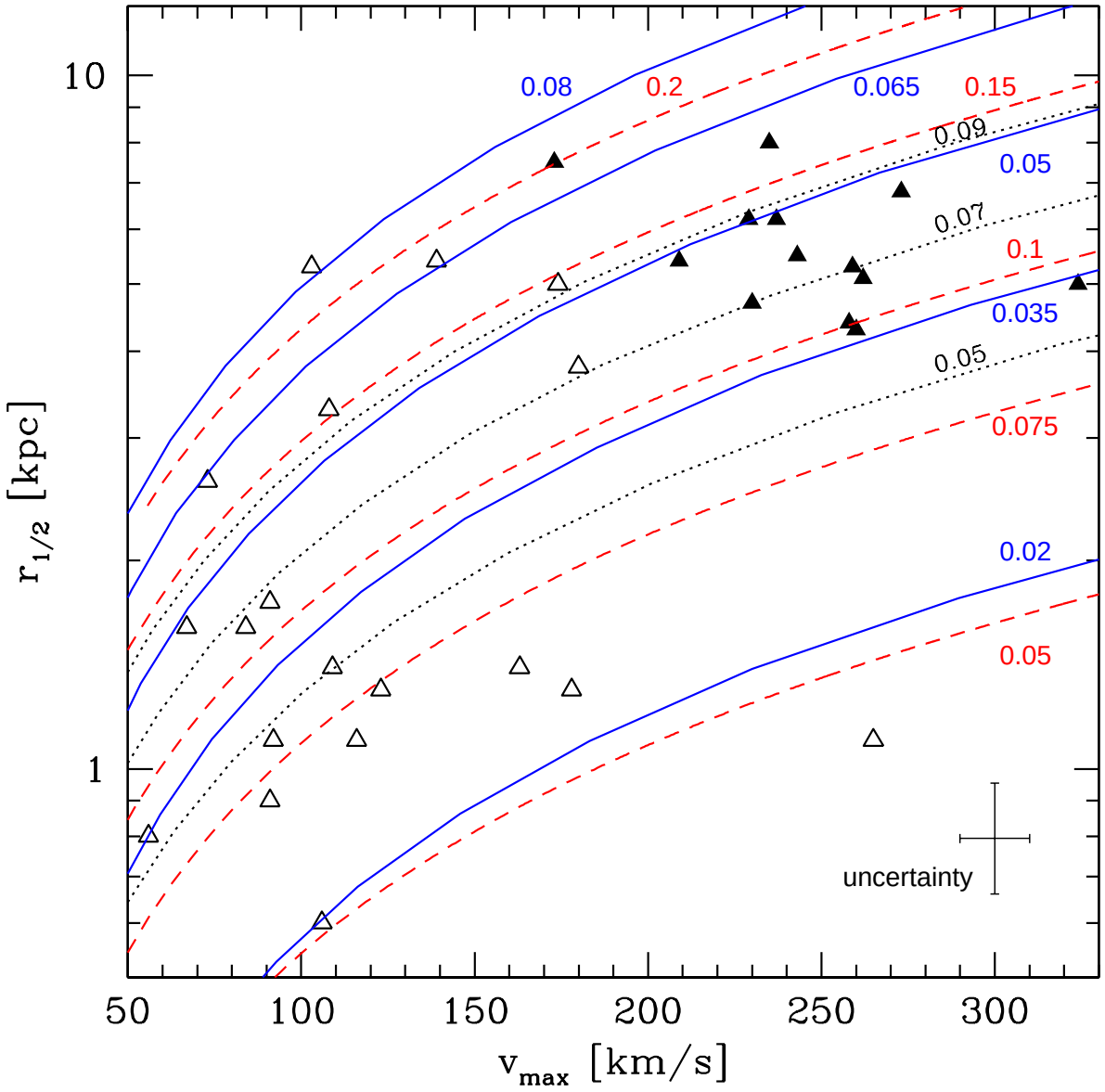

Fig. 1.— Triangles show the disk half-light radii $r_{1/2}$ versus the maximum rotational velocities v_{max} of the SINS high-redshift disk sample. Open triangles correspond to dispersion-dominated galaxies, filled triangles to rotation-dominated objects. The cross in the lower right corner indicates typical uncertainties. Red dashed lines show the theoretically predicted correlation between $r_{1/2}$ and v_{max} if pressure effects are neglected for various values of the disk spin parameter λ (red labels) and adopting a MMW model with a disk mass fraction of $m_d = 0.1$. Blue lines show MMW models including the effect of a pressure gradient and adopting $v_{max}/\sigma = 2$. The black dotted lines represent rotation-dominated galaxies with $v_{max}/\sigma = 5$, neglecting adiabatic dark halo contraction.

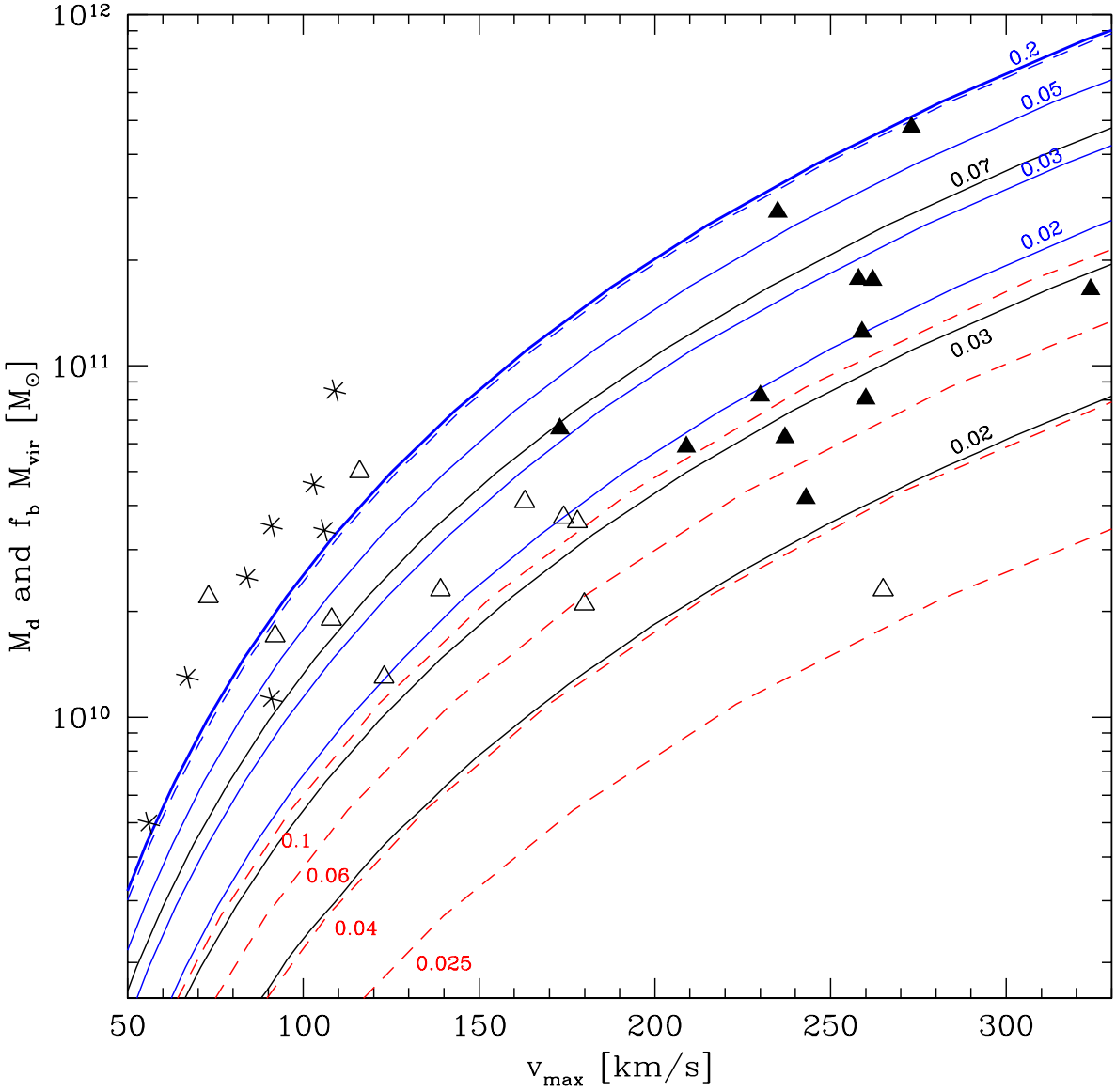

Fig. 2.— Open and filled triangles show the observationally inferred disk masses versus the maximum velocity of dispersion-dominated and rotation-dominated high-redshift SINS galaxies, respectively. The stars show extremely dispersion-dominated galaxies with $v_{max}/\sigma \leq 1.5$. The red dashed curves correspond to the maximum baryonic mass according to the standard MMW model, adopting a universal baryon fraction of f_b=0.17. Red labels indicate the corresponding disk λ parameters. The blue solid lines show the situation if turbulent pressure is taken into account, adopting $v_{max}/\sigma = 2$. The dashed blue curve next to the blue solid line labeled $\lambda = 0.2$ corresponds to $\lambda = 0.1$. Black curves correspond to MMW models with $v_{max}/\sigma = 5$, neglecting adiabatic contraction of the dark halo.

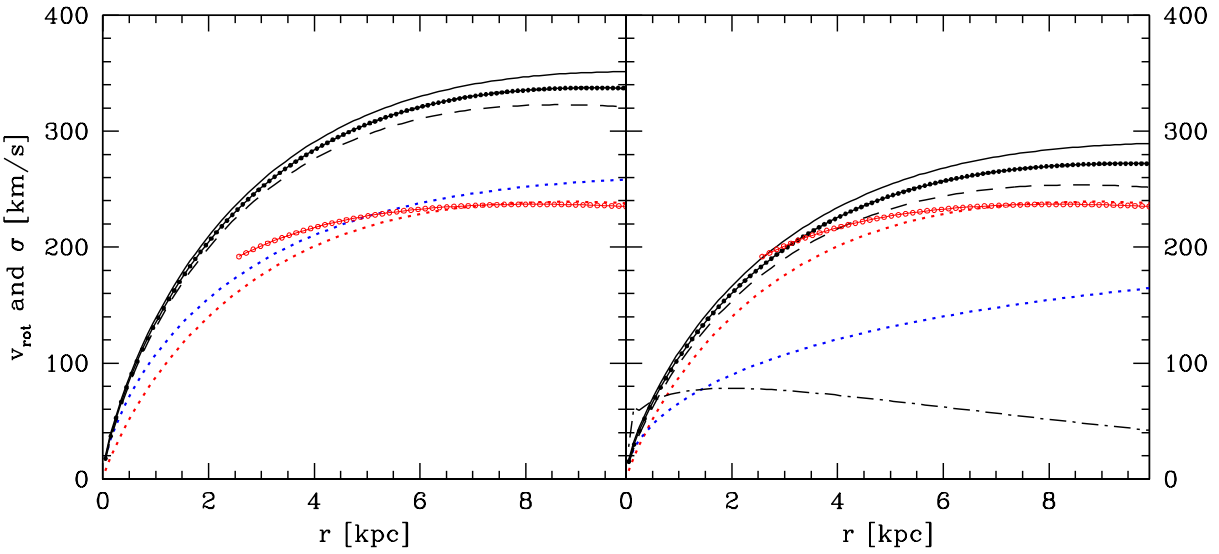

Fig. 3.— Open red circles in both panels show the inclination and resolution corrected intrinsic rotation curve of BzK-15504, derived from fitting the observed two-dimensional distribution of Hα velocities (Genzel et al. 2006). Only data points outside of 3 kpc are shown as the inner regions are affected by the central AGN and bar. The dotted red and blue lines in the left panel show the theoretically expected contribution of the disk and dark halo component, respectively, adopting a standard MMW model with adiabatic dark halo contraction. The combination of both curves leads to the zero-pressure total rotation curve (upper black line) that exceeds the observed maximum rotational velocity by more than 100 km/s. The black points and the dashed black curve correspond to the pressure corrected rotation curve, including pressure effects with a gas velocity dispersion of 45 km/s and 65 km/s, respectively. The right panel shows the situation without adiabatic dark halo contraction. Symbols and lines are the same as in the left panel. Now the resulting rotation curve is in much better agreement with the observations. The lower dot-dashed black curve shows the theoretically predicted velocity dispersion profile assuming a constant Toomre stability parameter of Q=1.

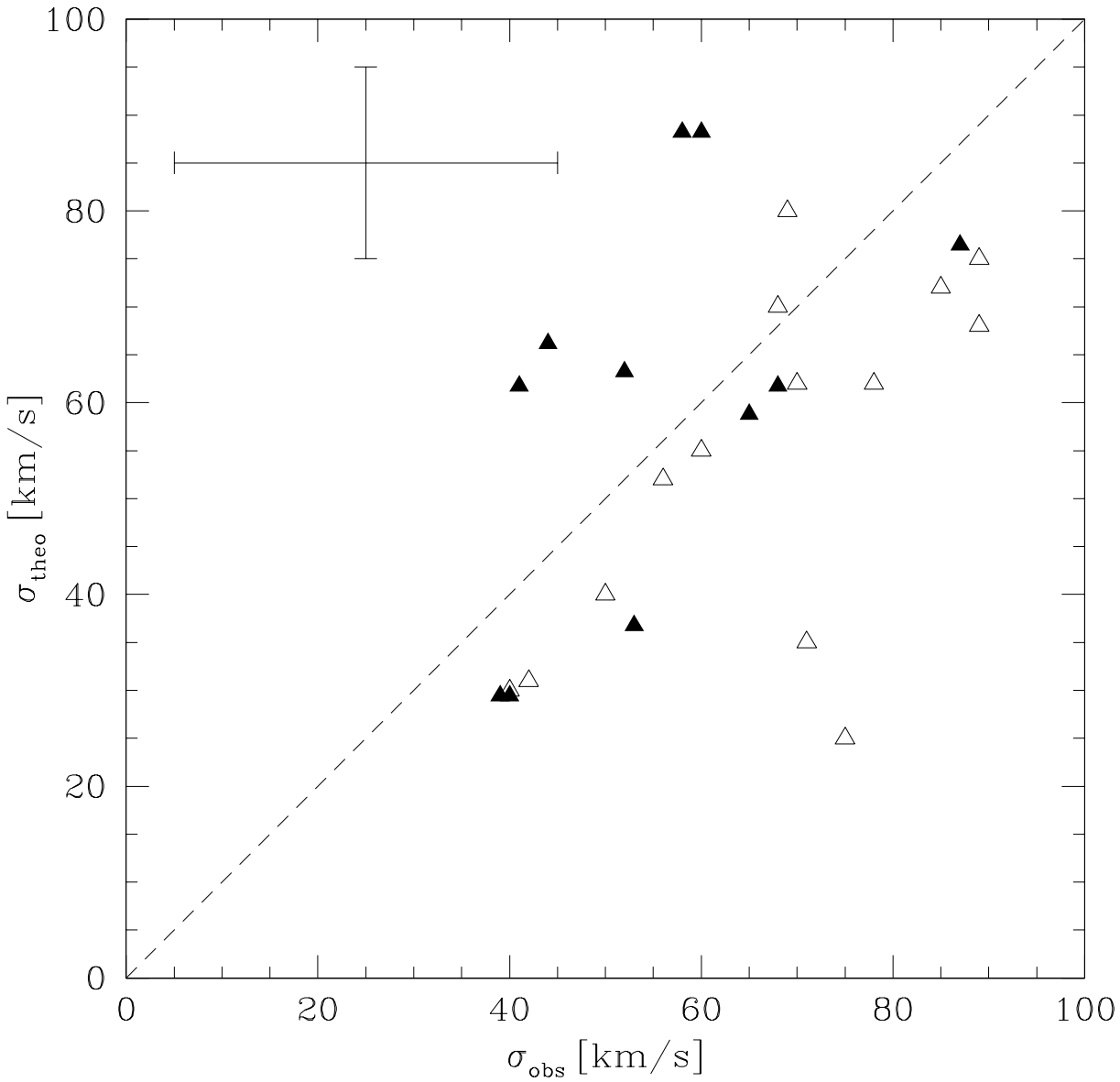

Fig. 4.— The observed velocity dispersion σ_{obs} of the SINS high-redshift galaxy sample is compared with theoretical expectations σ_{theo}, adopting a pressure-corrected MMW model without adiabatic halo contraction. Open and filled triangles correspond to dispersion and rotation-dominated systems, respectively. The error bar in the upper left corner indicates the observational uncertainties.